Optimizing (Augmenting) momentum resolution with a new fitting method.

Gregorio Landi,

Depart. of Physics and Astronomy, University of Firenze; INFN Sezione di Firenze

1. G. Landi, Nucl. Instrum. Meth. A **485**, 698 (2002) .
2. G. Landi, Nucl. Instrum. Meth. A **497** 511 (2003).
3. G. Landi, Nucl. Instrum. Meth. A **554** 226 (2005).
4. Gregorio Landi arXiv 1403.4273.
5. Gregorio Landi arXiv 1404.1968 and JINST 9 P 10006 2014.
6. Gregorio Landi arXiv 1606.03051.

The least squares method and the (so called) Gauss-Markov theorem

- **B.** best
- **L.** linear
- **U.** unbiased
- **E.** evaluation

Standard Axiom for the demonstration

:

Homoscedasticity: All the data must have identical variance.

Microstrips

Often used for microstrips $\sigma = [\frac{StripWidth}{S.N.R}]$.

This constant σ must be connected to a symmetry!.

Translation invariance?

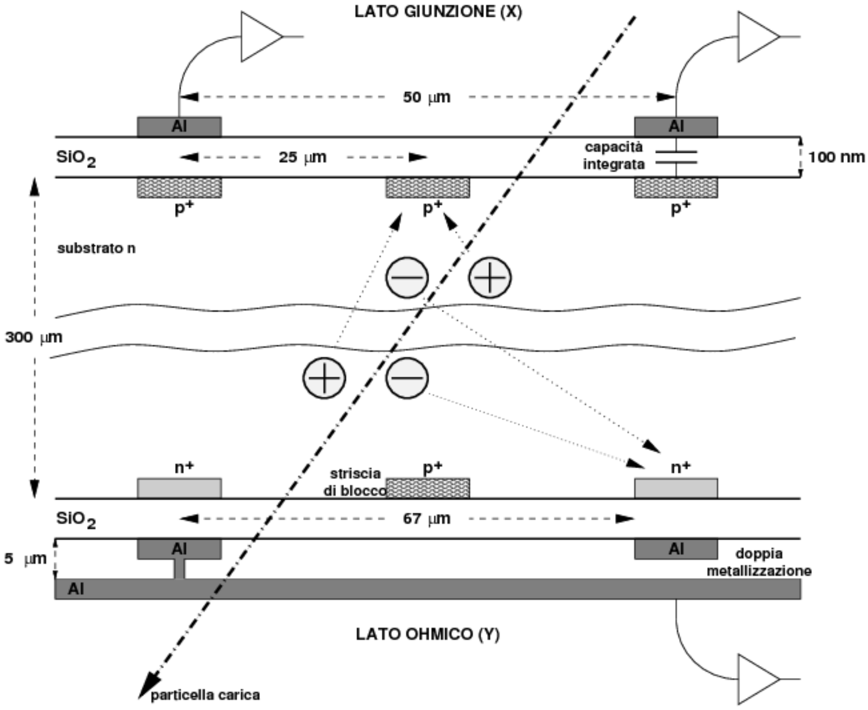

No translation invariance. At most periodicity!!!

Indications of heteroscedasticity: CMS muon tracker

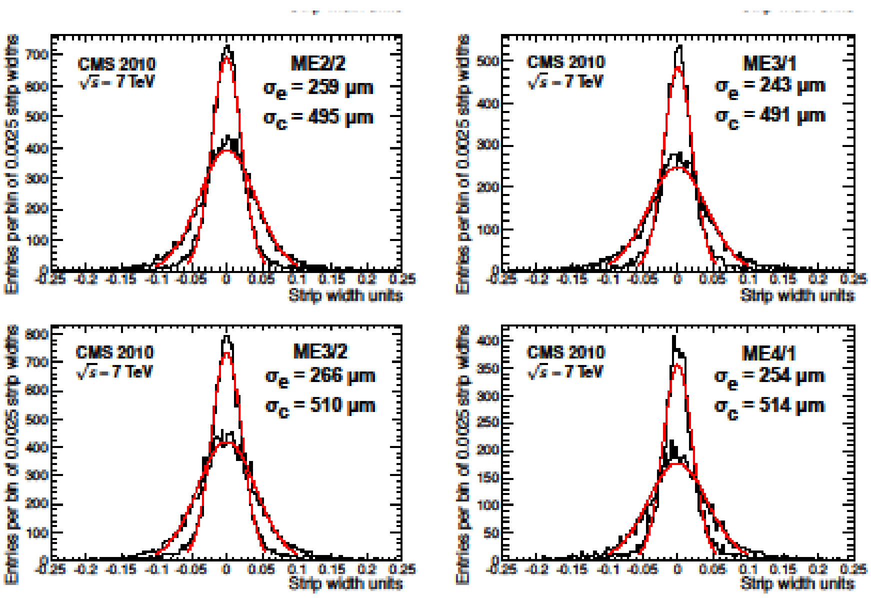

Simulations PAMELA-like ohmic-side

Very evident heteroscedasticity.

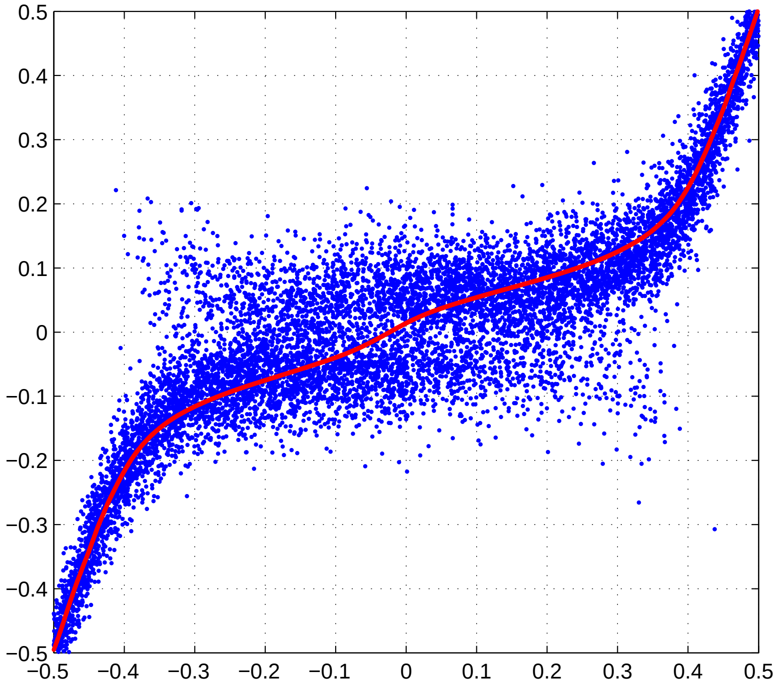

Even a set of (very) approximate PDFs, extracted from the data, gives an evident improvement of the track fits. (Maximum likelihood is obliged). The red line is the η_2-algorithm that correct the center of gravity (COG) systematic error.

A PDF for each measure should be known (Gauss 1821)

PDF for the two strip COG.

We follow an analogy with scattering amplitude in Quantum Mechanics. Completely different from the standard methods of Probability Theory (more than ten pages of integrals) .

$$x = \frac{x_1}{x_1 + x_2}\theta(x_1 - x_3) - \frac{x_3}{x_3 + x_2}\theta(x_3 - x_1)$$

$$P_{x_{g2}}(x) = \int_{-\infty}^{+\infty} \mathrm{d}\, x_1 \mathrm{d}\, x_2 \mathrm{d}\, x_3\, P(x_1, x_2, x_3)$$
$$\Big[\delta(x - \frac{x_1}{x_1 + x_2})\theta(x_1 - x_3) + \delta(x + \frac{x_3}{x_3 + x_2})\theta(x_3 - x_1)\Big] \tag{1}$$

The two δ integrations are expressed by:

$$\int_{-\infty}^{+\infty} \mathrm{d}\, z\, F(z - \nu)\, \delta(x \mp \frac{\nu}{z}) = F(\frac{\pm\nu}{x} - \nu)\, \frac{|\nu|}{x^2}\,. \tag{2}$$

And the PDF for the two strip COG becomes:

$$P_{x_{g2}}(x) = \frac{1}{x^2}\Big[\int_{-\infty}^{+\infty} \mathrm{d}\, \xi \int_{-\infty}^{\xi} \mathrm{d}\beta\, P(\xi,\, \xi\frac{1 - x}{x}, \beta)\, |\xi| +$$
$$\int_{-\infty}^{+\infty} \mathrm{d}\, \beta \int_{-\infty}^{\beta} \mathrm{d}\xi\, P(\xi,\, \beta\frac{-1 - x}{x}, \beta)\, |\beta|\Big]\,. \tag{3}$$

The random noise of the strips are independent. The mean values are correlated. For $P(x_i)$ the gaussian approximation is realistic.

$$P_i(x_i) = \exp\Big[-\frac{(x_i - a_i)^2}{2\sigma_i^2}\Big]\frac{1}{\sqrt{2\pi}\sigma_i}. \tag{4}$$

The integrations in $P(x)$ have no closed form. For small x approximation, one of the Gaussian PDF can be approximate as a Dirac δ-function. The other two Gaussian PDFs can be easily integrated, giving:

$$P_{x_{g2}}(x) = \frac{|a_2|}{\sqrt{2\pi}}$$
$$\Big\{\frac{e^{-(x-\frac{a_1}{a_1+a_2})^2\frac{(a_1+a_2)^2}{2\sigma_1^2(1-x)^2}}\big[1-\mathrm{erf}\big((\frac{a_3}{a_2+a_3}-x)\frac{a_2+a_3}{\sqrt{2}\sigma_3(1-x)}\big)\big]}{2\sigma_1(1-x)^2}+$$
$$\frac{e^{-(x+\frac{a_3}{a_3+a_2})^2\frac{(a_3+a_2)^2}{2\sigma_3^2(1+x)^2}}\big[1-\mathrm{erf}\big((\frac{a_1}{a_2+a_1}+x)\frac{a_2+a_1}{\sqrt{2}\sigma_1(1+x)}\big)\big]}{2\sigma_3(1+x)^2}\Big\}. \tag{5}$$

That can be used even for not too small x (the small parameter is $|x|\sigma_2/a_2 \ll 1$ and σ_2/a_2 is the signal-to-noise ration of the central strip)

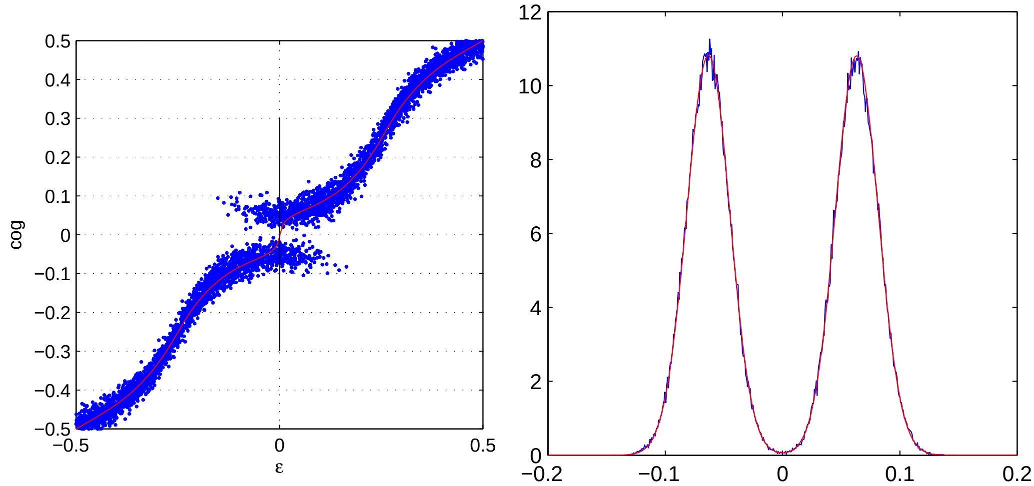

To obtain the PDF for each hit we have to insert the functional dependence from the impact point that is contained in the $\{a_i\}$ parameters. They become the functions $a_i(\varepsilon)$ where ε is the impact point.

The introduction of the functional dependence from the impact point

The filtering of the following distribution gives the functions $\{a_i(\varepsilon)\}$

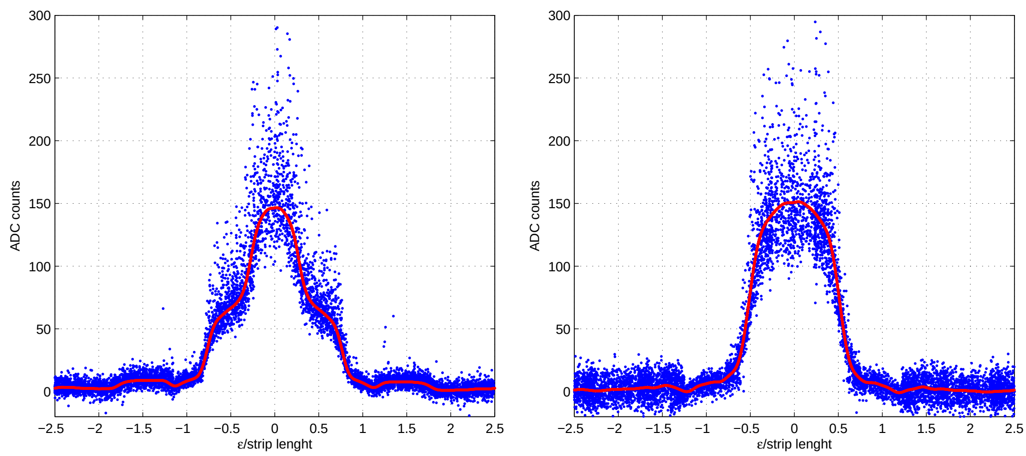

The sliding window

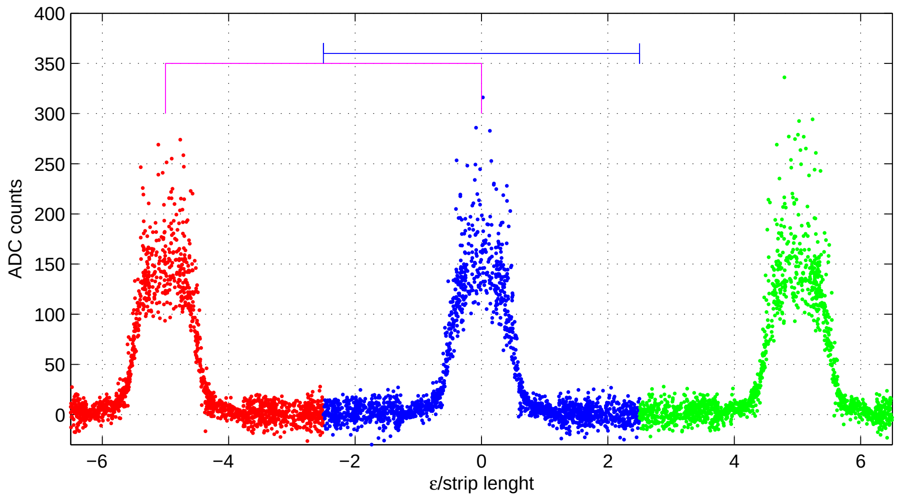

The PDF for each hit (automatically corrects even the COG_2 systematic error)

$$P_{x_{g2}}(x, E_t, \varepsilon) = \frac{F(a_1(\varepsilon), a_2(\varepsilon), a_3(\varepsilon), E_t, \sigma_1, \sigma_2, \sigma_3, x)}{x^2}. \tag{6}$$

Momentum reconstruction

Track definitions

$$
\begin{aligned}
\xi &= -R + \sqrt{R^2 - z^2} = \varphi(z) \quad p = 0.3 B_0 R \\
\xi_n &= \beta_n + \gamma_n z - \alpha_n z^2 = \varphi_n(z)\,.
\end{aligned} \tag{7}
$$

Maximum likelihood

$$
\begin{aligned}
&L(\alpha_n, \beta_n, \gamma_n) = -\sum_{j=6n+1}^{6n+6} \ln[P_{x_{g2}}(x(j), E_t(j), \psi_j(\alpha_n, \beta_n, \gamma_n)] \\
&\psi_j(\alpha_n, \beta_n, \gamma_n) = \varepsilon(j) - \varphi(z_j) + \varphi_n(z_j)\,.
\end{aligned} \tag{8}
$$

Definition of the effective σ

$$
\sigma_{eff}(i)^2 = \int_{\eta_2(i)-c_t}^{\eta_2(i)+c_t} P_{x_{g2}}(x(i), E_t(i), \varepsilon)\varepsilon^2 \, \mathrm{d}\varepsilon\,.
$$

The cuts c_t are optimized on the excellent hits and used for any other hit. Our first use of σ_{eff} was the initialization of the maximum likelihood search (in reality the minimum of $L(\alpha_n, \beta_n, \gamma_n)$ as usual).

σ_{eff} distribution

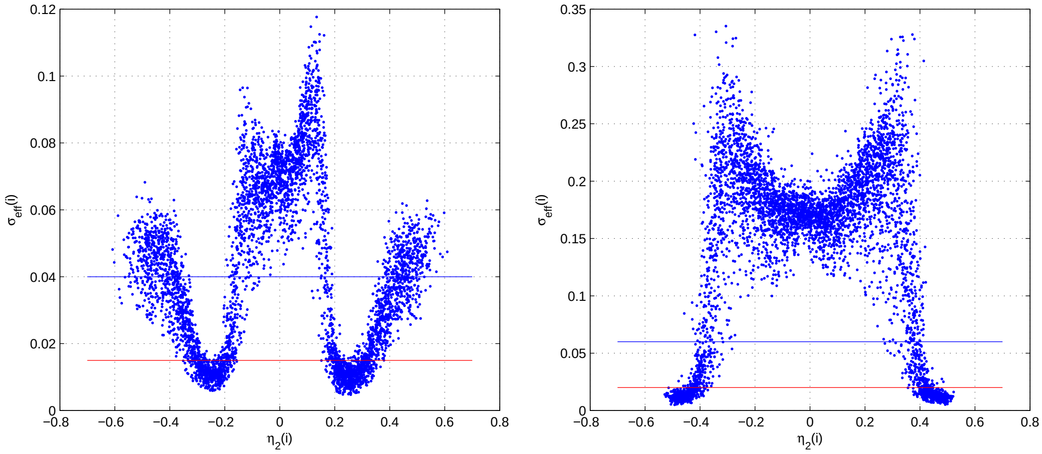

Momentum 350 GeV (floating side)

Differences from the exact positions and the reconstructed ones.

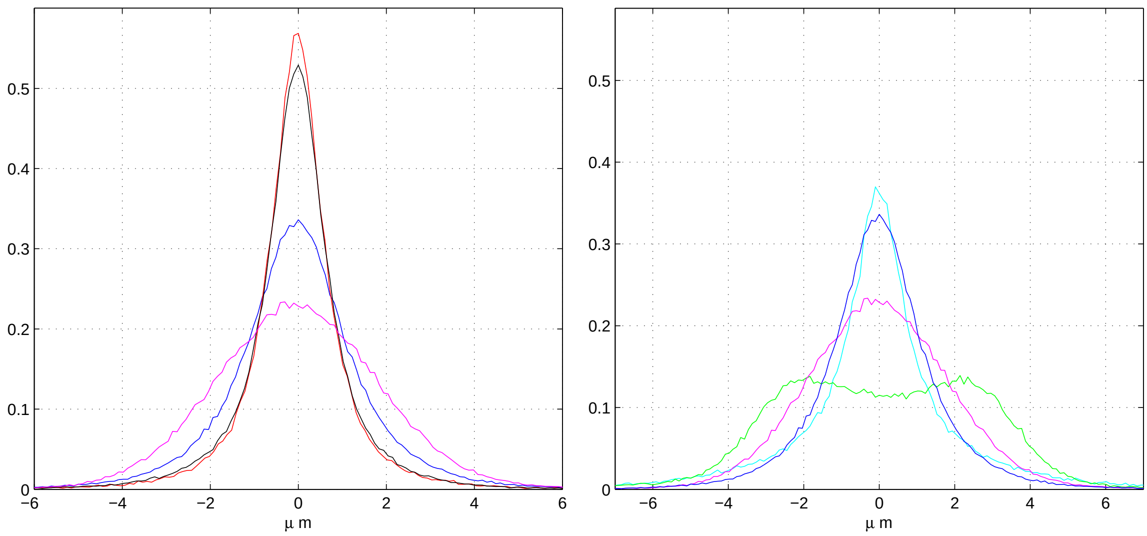

- Color Code
- **Red** Maximum likelihood evaluation
- **Black** weighted least squares σ_{eff}, position η_2

- **Blue** least squares, position η_2
- **Magenta** least squares, position COG_2

Momentum reconstruction, low noise floating strip side

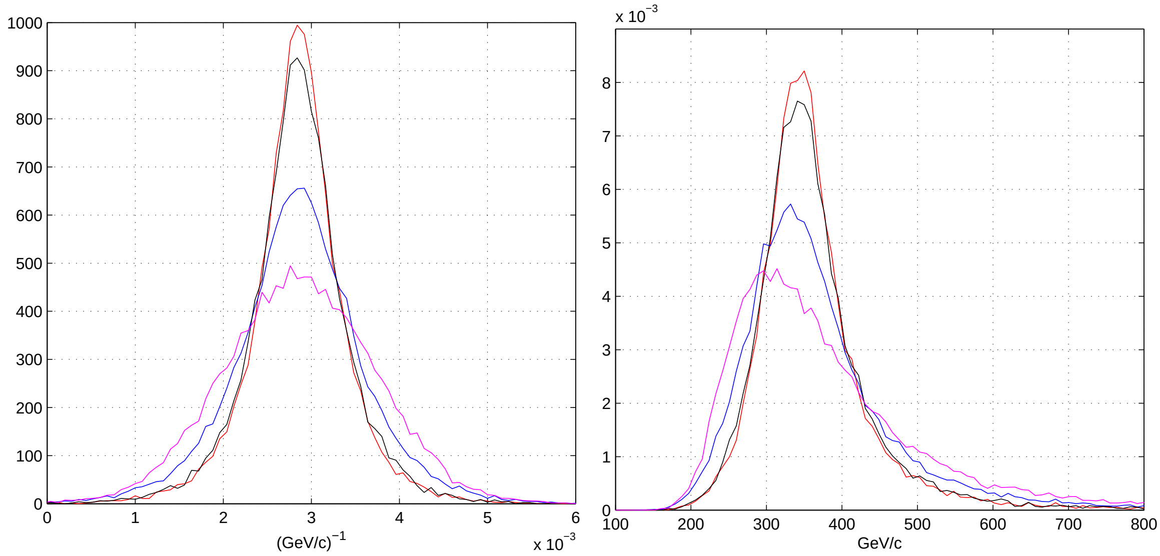

High noise side "Normal strips"

Incident Momentum: 150 GeV

The incident momentum must be reduced to have decente histograms of the reconstructed momenta

Differences from the exact positions and the reconstructed ones.

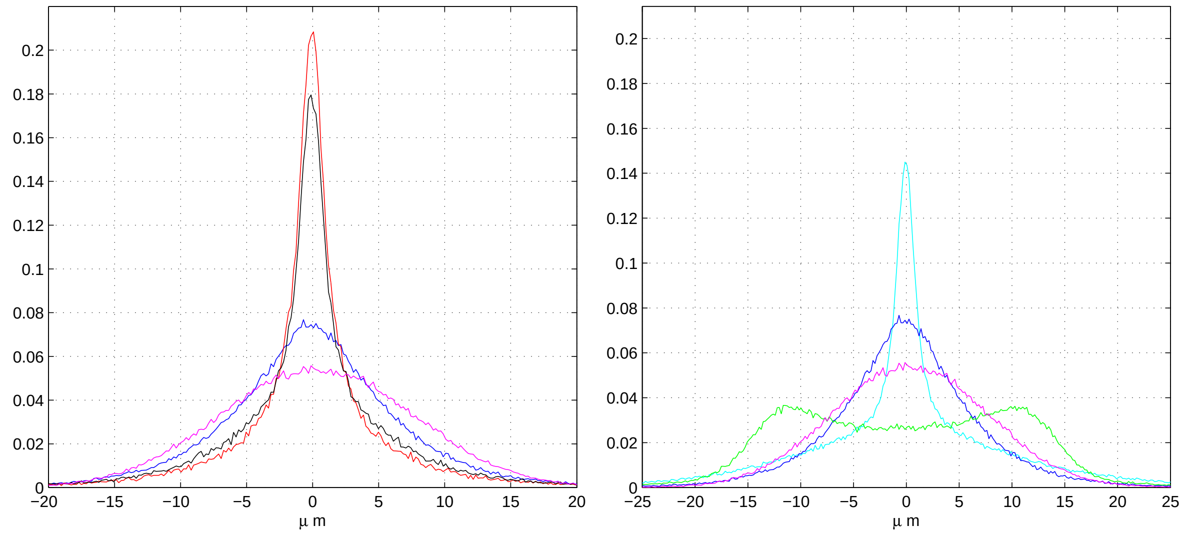

Momentum reconstruction high noise side normal strips

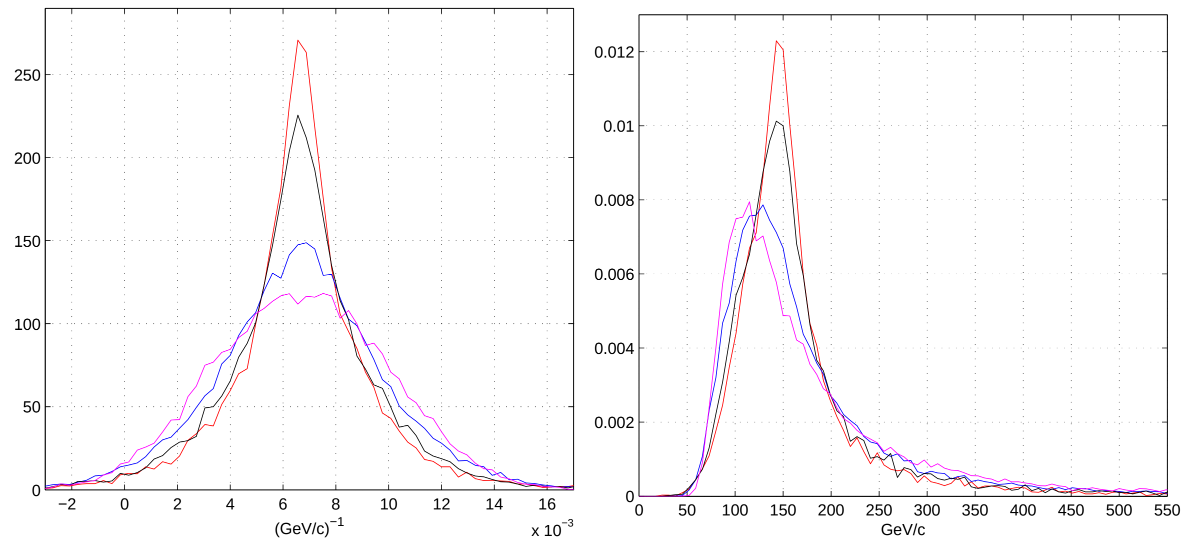

Comparison among various fits

To evaluate the increase of resolution we augment the effective magnetic field for the η_2 position least squares up to the overlap

with the Maximum Likelihood Evaluation

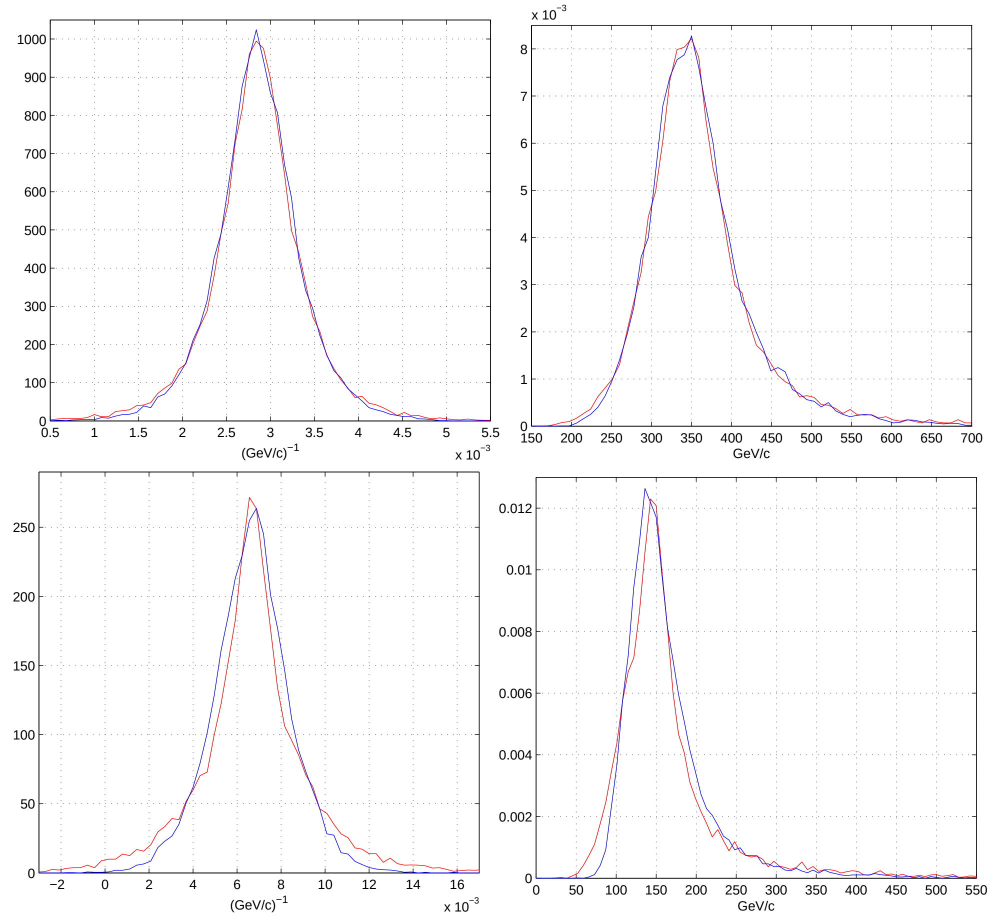

The two upper plots refer to low noise floating strip side. The magnetic field must be increased by a factor 1.5 for the overlap.

The two lower plots refer to the high noise normal strip side. The magnetic field must be increased by a factor 1.8 for the overlap.

Similar plots can be done for the COG_2-position least squares and the magnetic field increase must by a factor 1.8 for the low noise side and by a factor 2 for the high noise side.

- ——**Low noise floating strip side**
- η_2 position $B_{eff} = 1.5B_0$
- COG$_2$ position $B_{eff} = 1.8B_0$
- ——-**High Noise normal side**
- η_2 position $B_{eff} = 1.8B_0$
- COG$_2$ position $B_{eff} = 2.0B_0$

Increase of the signal-to-noise ratio to reach the overlap

- ——**Low noise floating strip side**
- η_2 position $\sigma = 4ADCcounts \Rightarrow 2.5ADCcountsr.m.s.$
- COG$_2$ position $====================$
- ——-**High Noise normal side**
- η_2 position $\sigma = 8ADCcounts \Rightarrow 3.6ADCcountsr.m.s.$
- COG$_2$ position $====================$

The plots are practically identical to those for the magnetic field. For the η_2 positioning (Low noise side) the signal-to-noise ratio must be increased of a factor 1.6.

For the η_2 positioning (High noise normal side) the signal-to-noise ratio must be increased of a factor 2.2.

Noise reduction has no effect on the COG$_2$ least squares. The COG$_2$ systematic error dominates the fit

The use of the COG as positioning algorithm moves the fit outside the domain of the Statistic.

The elimination of the systematic errors, as soon as they are "tabulated", is explicitly imposed by Gauss (1821) just to avoid "unpleasant results".

After the year 2002, the use of the COG in a fit must be considered outside the Gauss-Markov theorem

Different numbers of detecting layers

The presence of high quality hits suggests that they are the crucial elements of the resolution.

Thus, increasing the layer numbers, the probability of high quality hits grows with the layer numbers and similarly the resolution.

This grow is quite different respect to the least squares that grows, at most, as the square root of the layer numbers.

The layer numbers are increased from 3 to 8. Each result is shifted by a fixed step to avoid the overlaps.

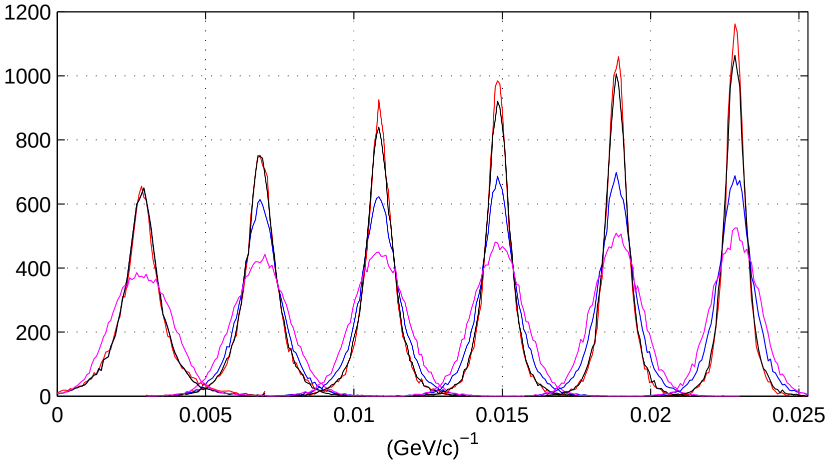

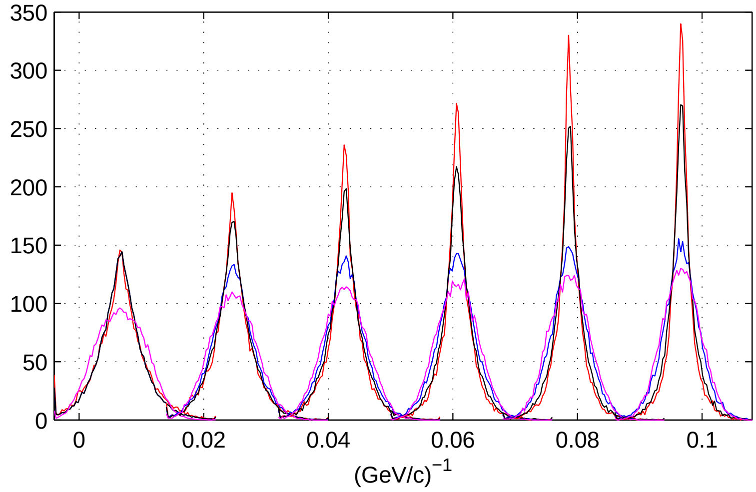

Tracks with a special hit combinations

Let us define (more or less arbitrarily) excellent hits and good hits.

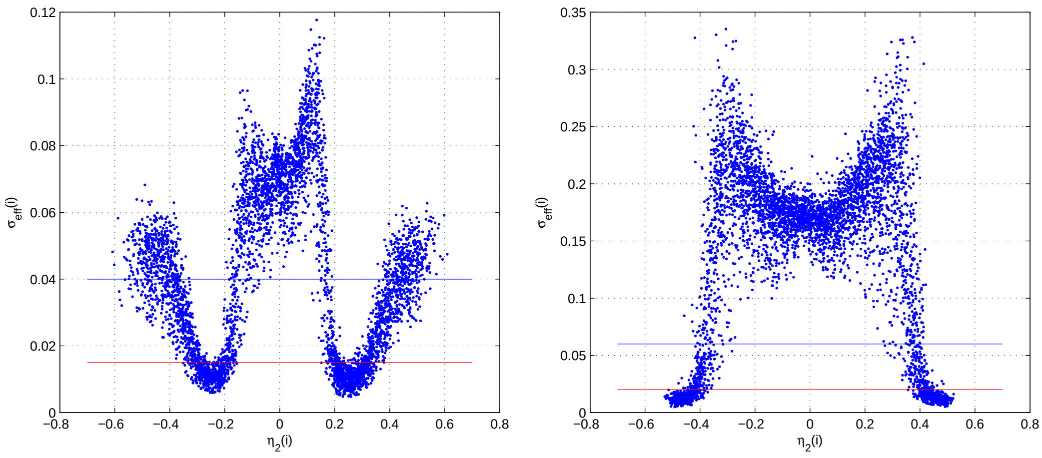

Below the red lines we have the excellent hits, below the blue lines and above the red we have the good hits.

Tracks with two excellent hits and three good ($16.1\,\%$). Low noise floating strip side

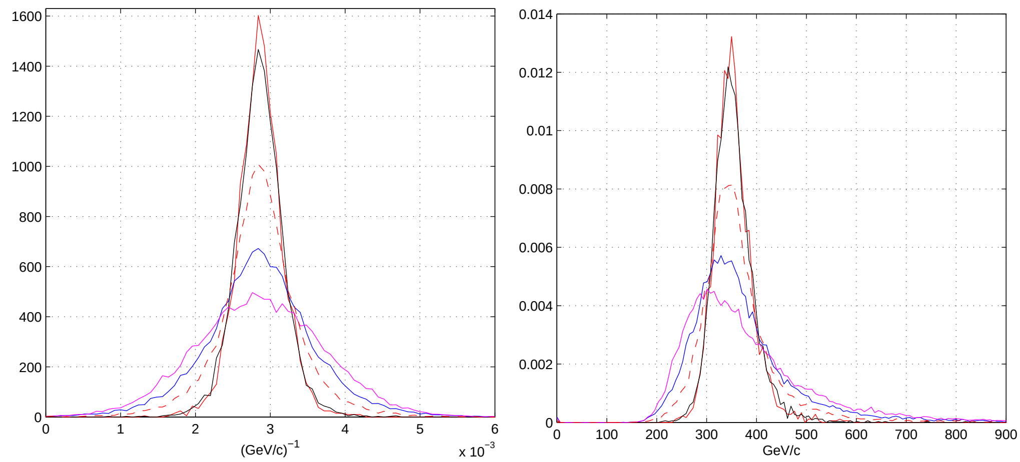

Tracks with two excellent hits and four other random ($25\,\%$). High noise normal strip side

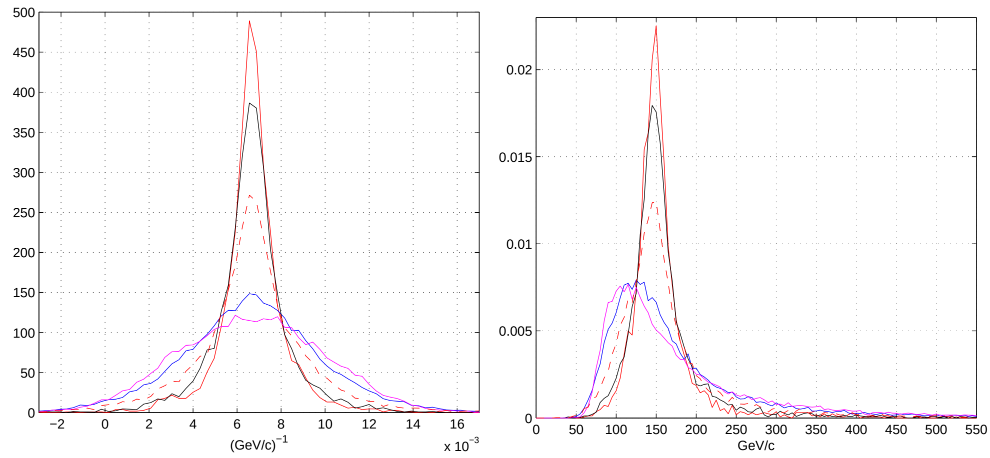

Heteroscedasticity gift for PAMELA

The homoscedasticity excludes couplings from the track variance and the resolutions of the fitted parameters.

What about heteroscedasticity?

Let us try. Select the track with the minimum variance up to a set of 25% and histogram the curvature and momentum distributions.

These distributions overlap our best results.